Trends in Plant Science

CellPress

Review

Advances in digital camera-based phenotyping of *Botrytis* disease development

Laura Groenenberg [1,6], Marie Duhamel [2,6], Yuling Bai [1], Mark G.M. Aarts [3], Gerrit Polder [4], and Theo A.J. van der Lee [5,*]

Botrytis cinerea **is an important generalist fungal plant pathogen that causes great economic losses. Conventional detection methods to identify *B. cinerea* infections rely on visual assessments, which are error prone, subjective, labor intensive, hard to quantify, and unsuitable for artificial intelligence (AI) and machine learning (ML) applications. New, often camera-based, techniques provide objective digital data by remote and proximal sensing. We detail the *B. cinerea* infection process and link this with conventional and novel detection methods. We evaluate the effectiveness of current digital phenotyping methods to detect, quantify, and classify disease symptoms for disease management and breeding for resistance. Finally, we discuss the needs, prospects, and challenges of digital camera-based phenotyping.**

Highlights

Digital phenotyping in plants offers enhanced accuracy and automation compared with traditional visual or manual methods. It enables early detection and quantitative analysis of phenotypic traits and can effectively be applied across various host plants and infection bioassays.

Utilizing red-green-blue (RGB) imaging alone significantly enhances measurements over visual and manual methods in the *Botrytis cinerea*–host interaction, but has limitations. To broaden the scope of insights, integrating additional sensors can provide a more comprehensive understanding of the interaction.

Digital phenotyping facilitates the imaging of a broader array of plant symptoms than can be observed by eye. During *B. cinerea* infection, multiple changes in reflectance and fluorescence spectra occur, which can be accurately quantified with digital phenotyping techniques.

Botrytis cinerea: an important plant pathogenic fungus

B. cinerea is a globally widespread fungal pathogen that causes gray mold disease, infecting nearly 600 plant genera and leading to significant crop losses both pre- and post-harvest due to spoilage and reduced yield and quality [1,2]. Its management is complicated by high spore production, fungicide resistance, and the formation of long-lasting soil-borne survival structures called sclerotia [3,4].

To reduce crop losses and control *B. cinerea*, curative disease control relies on applications of synthetic fungicides, which are being restricted due to the negative environmental effects and the emergence of multiresistant strains resulting from their frequent use [5]. Alternative methods to manage *B. cinerea* include the destruction of infected plant material and the control of plant spacing and humidity as well as the use of antagonistic microorganisms that can compete with or inhibit the growth of *B. cinerea* [6]. These measures are primarily implemented when symptoms are already apparent, and timely, early detection is crucial to enable prompt intervention such as the removal of infected plants and the targeted use of pesticides or antagonistic microorganisms [7]. Early detection can also offer insights into host–pathogen interactions including the identification of resistance and susceptibility, supporting resistance breeding. High-quality data are required for breeding as host resistance to *B. cinerea* is complex, involving multiple modes of action, and highly polygenic; often, each quantitative trait locus contributes only moderately to the overall resistance [8–11].

Traditional phenotyping methods for the detection of *B. cinerea* depend on visual inspection at critical stages of the crop production process, sometimes aided by microbiological, immunological, or molecular detection methods (Box 1 and Figure 1). However, visual inspection is subjective and thus linked to biased interpretation, and in addition requires substantial labor. By contrast, camera-based methods provide several advantages, including the ability to create nondestructive, high-throughput, objective, reusable, and standardized phenotypic data. This approach enables

[1]Laboratory of Plant Breeding, Wageningen University and Research, 6708PB Wageningen, The Netherlands
[2]Biointeractions and Plant Health, Laboratory of Genetics, Wageningen University and Research, 6708PB Wageningen, The Netherlands
[3]Laboratory of Genetics, Wageningen University and Research, 6708PB Wageningen, The Netherlands
[4]Greenhouse Horticulture, Wageningen University and Research, 6708PB Wageningen, The Netherlands
[5]Biointeractions and Plant Health, Wageningen University and Research, 6708PB Wageningen, The Netherlands
[6]Equal contributions

*Correspondence: theo.vanderlee@wur.nl (T.A.J. van der Lee).

Box 1. Conventional measurement practices

Conventional methods for early detection in asymptomatic tissues

Early detection, before conidial cluster formation or in asymptomatic tissues, is difficult but can be done by transferring leaf tissue to *Botrytis cinerea*-selective growth media [51–53]. Immunological detection methods such as lateral flow (or immunochromatic) devices [54] or ELISA [55] and in particular molecular methods such as quantitative **real-time PCR (RT-PCR)** [56] can be sensitive and specific. They are often able to detect *B. cinerea* during the early phases of the interaction. RT-PCR was shown to be more sensitive and accurate than plating for the detection of *B. cinerea* in symptomless grapes [57]. However, sampling of nonsymptomatic tissue intrinsically hampers the efficient use of these detection methods, as it is difficult to select the right material. A promising method to study the early phases of the disease is confocal spectral microscopy. Its high-resolution and ability to capture images at various depths within the specimen have been utilized to visualize early stages of *B. cinerea* infection [58]. This technique enables detailed examination of infection processes and cellular responses. Confocal microscopy is currently time-consuming and requires specialized expertise and equipment, and the throughput is limited. Therefore, confocal spectral microscopy is effective only when plants are inoculated and the inoculated sites are studied, and even then it would benefit from automation in data acquisition and automated analysis; for instance, when modes of action or specific processes such as conidial spore germination or penetration need to be identified and quantified.

Conventional detection methods in symptomatic tissues

Plating infected plant tissues on selective media such as *Botrytis* selective medium (BSM) [59] and monitoring colony morphology is a method to detect and identify *B. cinerea* once symptoms are visible. When conidia and conidiophores are developed, these can be captured on sticky tape and analyzed for the typical morphology of the conidiophores and conidia by microscopy. Previously mentioned methods are also all suitable to detect *B. cinerea* during symptomatic phases (3 and 4, see Figure 1 in the main text). In addition, several plant cellular changes related to *B. cinerea* infection can be observed by staining and magnification. The H_2O_2 level can be studied using diaminobenzidine and $CeCl_3$ staining [60]. Chloroplast disintegration, occurring during *B. cinerea* infection, can be observed by examining chloroplast number and structure with a light microscope with 40× magnification. Transmission electron microscopy on ultrathin sections can be employed to identify alterations in the ultrastructure of the chloroplasts. The efficiency of the ascorbate–glutathione system in response to the oxidative burst during infection can be assessed by examining glutathione and ascorbate level using **immunogold labeling** followed by transmission electron microscopy [60]. However, these techniques visualize symptomatic phenomena at the nanoscale and are not suitable for higher-throughput experiments. In addition, these phenomena are not specific to *B. cinerea* and can be observed with other plant pathogens.

automated disease detection and better phenotypic data on disease symptoms to dissect the genetic components determining plant resistance and susceptibility [12]. Digital information can also be used for AI and ML applications that would enable advances in automated detection, quantification, and classification of the disease symptoms, that can be deployed in **quantitative trait locus (QTL)** (see Glossary) analysis and disease management strategies.

This review focuses on the technologies for imaging different stages of *B. cinerea* disease development (Figure 1 and Box 2) in whole plants, detached leaves, and post-harvest fruits and vegetables. While environmental conditions are crucial in influencing *B. cinerea* pathogenesis, this review is centered on (early) symptom detection rather than environmental monitoring, using the term '**digital phenotyping**' to refer to camera-based imaging technologies. We provide insights into the application of digital phenotyping to monitor and quantify different aspects of the interaction between *B. cinerea* and its host, which will facilitate better management of this disease and underpin breeding for *B. cinerea* resistance. Finally, we identify current knowledge gaps while also offering guidance for future research in this area.

Digital camera-based phenotyping of *B. cinerea*

Digital phenotyping utilizes cameras detecting the reflectance or fluorescence across a range of wavelengths, extending from shorter wavelengths like gamma- or **X-rays** to long ones such as radio waves. The cameras applied for imaging in this review operate within the wavelength range from 380 nm, marking the start of the visible spectrum, to 14 µm, the end of long-wave IR, also known as thermal camera detection. These wavelengths are associated with the chemical composition of leaves, such

Glossary

Chlorophyll fluorescence imaging (CI): measures chlorophyll fluorescence to assess photosynthetic efficiency and response to stress.
Chlorosis: reduction of chlorophyll often resulting in the yellow appearance of the leaves.
Classifier: a ML algorithm that automatically categorizes data into one or more predetermined classes.
Computed tomography (CT): an imaging technique that uses X-rays to create detailed cross-sectional images of an object. By combining these slices, a 3D representation can be reconstructed, allowing precise internal visualization.
Conventional detection: detection methods that have been used often over the past decades, such as visual observations.
Digital phenotyping: the use of sensor technology to measure plant traits and characteristics digitally. Digital phenotyping of plants primarily relies on imaging techniques, but also involves automated data collection and processing.
***Fv/Fm*:** measures the quantum yield of the primary PSII photochemistry in dark-adapted photosynthetic samples [50]. The variable chlorophyll fluorescence is divided by the maximum chlorophyll fluorescence. This ratio is an indicator of plant photosynthetic performance.
Genome-wide association study (GWAS): tests a wide range of genomic variants to identify those that are statistically associated with a particular phenotypic trait.
Immunogold labeling: in this technique, antibodies are used to bind, on biological material, particles of colloidal gold that are easily visible using electron microscope.
Near-IR (NIR): a subset of the IR band of the electromagnetic spectrum, covering the wavelengths between 700 and 1400 nm.
Necrosis: death of plant tissue; visual symptoms often appear brown or black/gray.
Quantitative trait locus (QTL): a DNA region correlated with a specific phenotypic trait that varies within a population.
Real-time PCR (RT-PCR): combines reverse transcription of an RNA sample into DNA and amplification of a target fragment of this DNA.

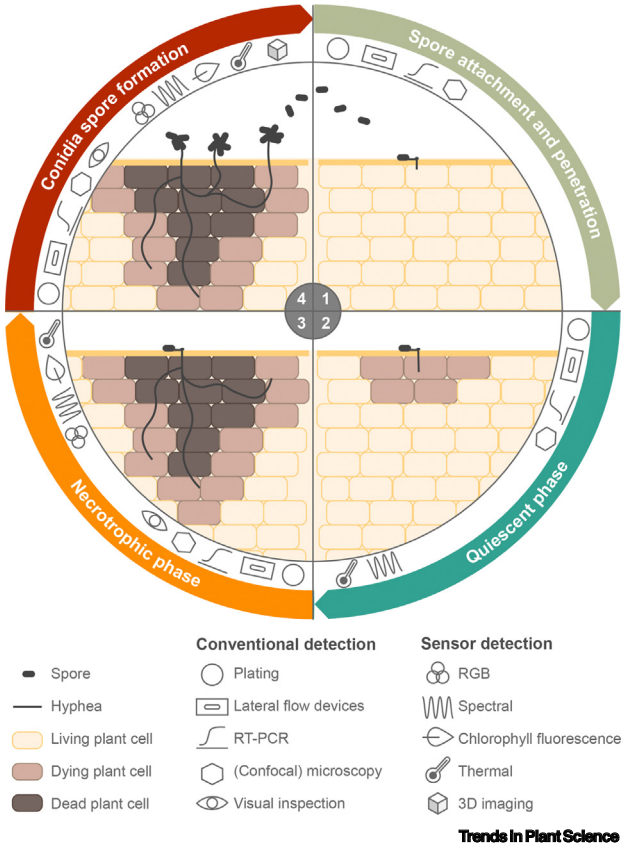

Figure 1. The four phases of *Botrytis cinerea* disease progression, with **conventional detection methods** and sensor-based detection methods indicated. (1) Attachment of conidial spores and subsequent penetration of the host. This process encompasses various modes of entry; namely, (i) through appressoria, (ii) via infection cushions, and (iii) utilizing stomata and wounds. (2) The latent phase, during which *B. cinerea* grows but no visual symptoms appear on the host. (3) The necrotrophic phase, during which the pathogen establishes primary lesions and further develops these lesions. This phase is characterized by chlorosis and necrosis. (4) The sporulation phase, in which *B. cinerea* generates conidiophores containing the asexual conidial spores. These spores disperse locally by run-off water and more distantly by air, land on new, often adjacent host surfaces, and recommence the life cycle. Several conventional and digital phenotyping methods can be applied to detect and quantify disease expression in these four phases. Not all methods apply to each phase. Abbreviations: RGB, red-green-blue; RT-PCR, real-time PCR.

Red edge (RE): the portion of the electromagnetic spectrum covering the wavelengths between 670 and 760 nm.
Red-green-blue (RGB) imaging: captures and displays images using the red, green, and blue color channels.
Short-wave IR (SWIR): corresponding to the wavelength band of light between 900 and 2500 nm.
Spectral imaging: includes MSI and HSI (at the pixel level) and covers a broad range of wavelengths, typically from UV to IR.
Thermal imaging: performed by recording radiation emitted in the thermal IR range (8–14 μm).
Visible to NIR (VNIR): the visible and NIR portion of the electromagnetic spectrum covering the wavelengths between approximately 400 and 1100 nm
X-rays: a form of electromagnetic radiation (wavelength in the range 0.01–10 nm) that can penetrate various materials. They are commonly used to create images of the internal structure of objects.

as chlorophyll, nutrient, and water content [13]. The cameras most used for digital phenotyping are red-green-blue (RGB) cameras, cameras that specifically detect chlorophyll by fluorescence, multi- or hyperspectral cameras, and thermal cameras (Figure 2). The term hyperspectral imaging (HSI) for spectroscopy at the pixel level is debatable, and 'imaging spectroscopy' or '**spectral imaging**' without the use of ambiguous adjectives is preferred [14]; however, in line with most of the studies cited in this review, we have included the term HSI. For more details on the specificity and various limitations of the methods applied in various other pathosystems, readers are also referred to Tanner *et al.* [15].

Thermal imaging

Thermal cameras can obtain the spatial distribution of the object's temperature based on the IR radiation naturally emitted by objects in the thermal IR range (8–14 μm) (Figure 2C). The impact of *B. cinerea* infection on transpiration can be detected with such thermal cameras, as related alterations of the stomatal conductance are linked to a modification of the temperature at the lesion site [16]. This allowed the detection of presymptomatic tissues infected with *B. cinerea* in, for example, common bean leaves (*Phaseolus vulgaris*) [17] and rose petals [18,19]. However, in rose petals early symptom detection varied: Jafari *et al.* [18] reported a decrease in temperature in presymptomatic tissues, while Ha *et al.* [19] observed an increase. This discrepancy may be attributed to several factors, including environmental conditions, inoculation methods, imaging setup and sensitivity, and the measurement accuracy of the thermal sensor. Additionally, the type of lesions developed can impact the temperature, as water-soaked lesions tend to exhibit lower temperatures than healthy areas [18]. An advantage of **thermal imaging** is that it is not dependent on

Box 2. Infection process and physiological changes to plant cells

In this review, we differentiate among four phases of disease progression (see Figure 1 in the main text). The duration and infection mechanisms at each phase can vary, depending on plant species and tissue types.

During the first phase, conidia land on the host surface. Germination relies on humid conditions; in the absence of water droplets, relative humidity should generally be higher than 90% [61]. On germination, *Botrytis cinerea* enters the host through stomata or wounds or by penetrating the cuticle using infection cushions or an appressorium-like structure. *B. cinerea* secretes lytic enzymes that degrade host components [62]. It has been suggested that *B. cinerea* relies partly on physical force, in addition to chemical degradation, to overcome host defenses [63]. During infection, *B. cinerea* releases cell death-inducing proteins (CDIPs), triggering plant cell death and immune responses, potentially leading to hypersensitive response and necrosis [64]. In successful infections, small RNAs, coded by dicer-like *B. cinerea* genes, potentially suppress the host autophagic response. During the second phase, *B. cinerea* enters a latent stage, accumulating biomass without causing symptoms [65]. *B. cinerea* secretes metabolites such as botrydial botcinolide, oxalic acid, and enzymes that degrade the plant cell wall for the absorption of nutrients. These compounds initiate apoptosis in susceptible hosts. Depending on environmental conditions, host physiological state, and tissue type, *B. cinerea* may remain in this second phase, with growth either arrested or continuing endophytically in the apoplast [52,53,66]. The second phase is often observed in berry fruits, where infection can be halted until the flowering stage. Alternatively, infection on the fruits may lead to infection symptoms when fruits reach a certain maturity [67,68]. *B. cinerea* infection can also arise from infected seeds [52,53], in which case a long quiescent phase can occur.

During the third phase, symptoms start to develop. Early visible signs are the development of chlorotic areas followed by necrosis. The host accumulates reactive oxygen species (ROS) around the cell walls penetrated by the fungus, inside the cell, and in the plasma membrane. H_2O_2 will be generated around the fungal hyphae and accumulates in the cell walls. Accumulation of H_2O_2 in the mitochondria and chloroplasts results in chlorosis. Finally, H_2O_2 accumulation in the cytosol and nuclei leads to disintegration of the cytoplasm and necrosis. H_2O_2 is detoxified in plants by two main antioxidants, ascorbate and glutathione. When infection progresses, the ascorbate–glutathione ROS detoxification system efficiency decreases rapidly, leading to an oxidative burst and disintegration of the chloroplasts [60,68,70].

The fourth phase of a necrotrophic infection is rapid decomposition of plant cells and an increase of fungal biomass. Under suitable environmental conditions, the fungus will generate asexual reproductive organs (conidiophores) which produce massive amounts of conidial spores. These spores may result in new infections, and therefore timely disease detection of *B. cinerea* is critical to avoid spread [71].

illumination of the object; measurements are thus feasible in the dark or light. However, environmental conditions such as ambient and reflected temperature, humidity, plant canopy architecture, and leaf angles can strongly affect thermal images. Thermal imaging is therefore challenging for data acquisition as these physical parameters lead to nonuniformity of the imaging and may be difficult to correct.

RGB imaging

RGB imaging measures the plant surface reflectance over red, green, and blue wavelengths, which belong to the visible spectrum, and relates directly to visual observations (Figure 2A). In contrast to visual observation, RGB imaging provides quantifiable pixel data for calculations such as lesion size. Recent advances have integrated RGB with automation and ML to enhance throughput [20–22]. Currently, lesion size measured from the beginning of phase 3 (Figure 1) is a good indicator for susceptibility and resistance, which can be measured relatively early (24 h after infection). At later stages during the interaction, lesion size can be used as a trait to quantify resistance.[23] Use of RGB-derived lesion size alone has successfully facilitated **genome-wide association studies (GWASs)** in *Arabidopsis thaliana* [23]. Moreover, Fordyce *et al.* [24] demonstrated that RGB imaging can characterize a significantly greater number of parameters, including lesion shape, size, color, and texture (Box 3). These parameters could contribute to a more comprehensive understanding of traits recorded for GWASs. Furthermore, time-lapse imaging enables the assessment of additional parameters such as lesion growth rate, disease incidence, and progression over time in strawberry plants [25], as well as metrics like break time, intermediate-stage duration, acceleration, and late-stage lesion average expansion rate in beans and *Nicotiana benthamiana* [26]. This comprehensive characterization can enhance our

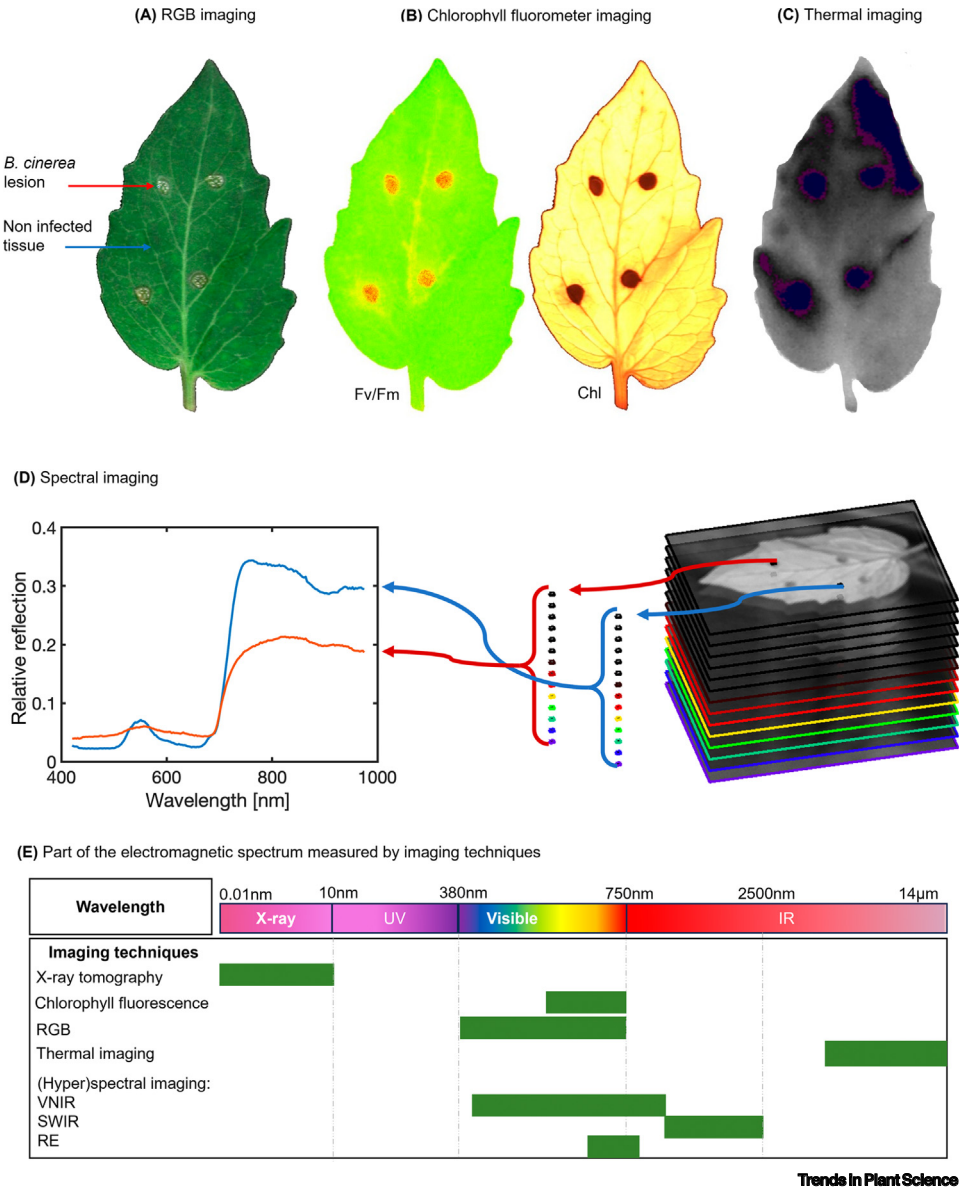

Figure 2. Different types of camera measurements for the same *Botrytis cinerea* lesion. A tomato detached leaf (*Solanum lycopersicum* Moneymaker) was inoculated with four droplets of 10 µl of *B. cinerea* conidial spore solution (10^6 spores/µl) and measured at 48 HPI (PlantExplorer PRO; PhenoVation, Wageningen, The Netherlands). (A) Red-green-blue (RGB) measurement. (B) Chlorophyll imaging. Here, the lesions are visible on *Fv*/*Fm* (indicator of plant photosynthetic performance) and chlorophyll content (Chl) images. The four lesions have a lower *Fv*/*Fm* and chlorophyll content than the healthy part of the leaf. (C) Thermal measurement [FLIR A655sc long-wave IR (LWIR) thermal camera]. The gray gradient represents the temperature gradient; darker areas are colder than light areas. (D) Spectral measurement (Specim FX10 line-scan hyperspectral camera that operates between 400 and 1000 nm). The red curve is the spectral reflectance curve from the *B. cinerea* lesion; the blue curve is the spectral reflectance curve from a healthy part of the tomato leaf. (E) The fraction of the electromagnetic spectrum that can be measured by the different imaging techniques. Abbreviations: RE, red edge; SWIR, short-wavelength IR; VNIR, visible to near-IR.

understanding of the interaction between *B. cinerea* and its host. Finally, RGB imaging has shown promise in distinguishing between pathogens, including *B. cinerea* in strawberry fruits [27], although further investigation is required for applications in which symptoms are less severe. The

Box 3. Impact of plant physical structures on *Botrytis cinerea* infection

The structure of plant leaves can have significant effects on the development of *B. cinerea* lesions. The use of digital phenotyping may assist with connecting changes in those features to *B. cinerea* infection. For instance, plant leaf or fruit surface characteristics can influence the attachment and penetration of *B. cinerea* spores. The presence, density, and type of trichomes or a waxy cuticle on the leaf surface can affect the ability of the pathogen to adhere to and enter the plant tissue. In *Arabidopsis thaliana*, trichomes have been shown to facilitate the adhesion of *B. cinerea* to the leaves [72], while in tomato a higher number of and longer type III non-glandular trichomes increased plant resistance [73]. Trichome types and number can be observed using micro X-ray CT or a stereomicroscope, for instance.

Furthermore, a lower cuticular wax level in *A. thaliana* is linked to a higher resistance to *B. cinerea* [74], and Liu *et al.* [75] showed that, for blueberry fruits, a higher level of wax increases the fruit resistance to *B. cinerea*. Leaf cuticular waxes can be studied with spectral methods, as their presence affects light reflection [76].

Stomatal density and opening also play a role in infection. Plants regulate stomatal closure and opening rate in response to environmental conditions via phytohormones such as abscisic and salicylic acids, affecting also their susceptibility to *B. cinerea* infection [77,78]. *B. cinerea* can use stomata as entry points. The density of stomata and their opening, including their aperture size, influence the access of the pathogen to the interior of the leaf. Stomatal guard cells play an important role in the plant defense system. Linking stomatal density and conductivity to *B. cinerea* infection can be performed with the help of a hand-held and confocal microscope but also by thermal imaging [79].

Leaf anatomy impacts the ability of *B. cinerea* to penetrate and colonize plant tissues. More complex leaf structures may provide physical barriers that limit the progression of the pathogen; the thickness and number of cell wall layers are important factors [80].

Senescence or aging of leaves often results in higher susceptibility to *B. cinerea* infection [81]. Changes in leaf physiology during senescence, including alterations in cell wall composition and nutrient availability, can create a more favorable environment for the pathogen. Meng *et al.* [82] showed that strawberry leaf resistance against *B. cinerea* increases from 1- to 4-week-old leaves and decreases again in 5-week-old leaves. Leaf shape and age can be monitored utilizing 3D imaging to look at the changes in leaf morphology linked with the infection; it can also help to focus on the leaf layer that is most susceptible to the pathogen.

reviewed studies indicate that RGB imaging cannot detect *B. cinerea* in early infection phases, limiting its use to symptomatic detection.

Chlorophyll fluorescence imaging (CI)

CI provides information on plant chlorophyll by measuring the light re-emitted at a lower wavelength after illumination. This can be used directly to measure the chlorophyll content but also to quantify the efficiency of photosynthesis by estimation of the ***Fv/Fm*** ratio. *Fv*/*Fm* has been successfully used as a marker for biotic and abiotic stress (Figure 2B). Using CI, **chlorosis**, **necrosis**, and the related changes in photosynthetic activity have been observed in leaves of several infected plant species such as tomato and strawberry [28–30]. CI of *B. cinerea* infection can be performed at different scales, such as the leaf level with a detached leaf assay, on whole plants in a greenhouse, or on produce such as grapes of flowers. Following pathogen inoculation, CI and segmentation track disease progression by measuring changes in fluorescence and categorizing pixels into background, healthy, chlorotic, necrotic, and low-photosynthesis areas over time. This method can be combined with other types of imaging such as RGB, as performed in the study from Pavicic *et al.* [31], or multispectral imaging (MSI) by Wang *et al.* [30].

MSI and HSI

MSI and HSI (Figure 2D) capture the reflectance properties of plant surfaces across a range of spectral bands, from **visible to near-infrared (VNIR)** (400–1000 nm) and **short-wave (SWIR)** (1000–2500 nm). This method enables the detection of spectral differences linked to physiological and pathological states at the leaf, flower, fruit, and whole-plant levels. By utilizing spectral sensors targeting VNIR and/or SWIR, the reflectance of healthy and *B. cinerea*-infected plant surfaces is measured across multiple spectral bands. Comparing the reflectance spectra allows the identification of wavelengths indicative of pathogen infection and aids in

disease quantification and classification (Figure 2D). Studies in (detached) leaves show that **NIR** and the red edge (RE) can be informative bands in differentiating infected and mock-inoculated regions. For example, Fahrentrapp *et al.* [32] revealed that infected leaves exhibited lower reflectance in these bands, enabling the identification of gray mold as early as 9 h (phase 1) post-infection in time-course experiments involving detached tomato leaves inoculated with *B. cinerea*.

To further understand the interaction between *B. cinerea* and its host, reference parameters such as soluble solid content, total phenolic content, and total anthocyanin content can be used as reference parameters. Some of these effects could be related to the early phases such as phase 1 and phase 2 (Figure 1) and hold promise for nonsymptomatic tissue detection. For example, Siedliska *et al.* [33], after inoculating individual fruits, could make a distinction between healthy versus infected strawberry fruits before visible symptoms appeared (phase 2, Figure 1) and accurately classify the phase of infection development using 19 characteristic wavelengths in the 617–2332 nm range, associated with carbohydrate, phenolic compound, anthocyanin, sugar, and water content. In another study with detached tomato leaves [34], HSI was utilized to predict the activity of peroxidases (PODs), a group of enzymes that is known to enhance plant defense mechanisms against pathogens. Although Kong *et al.* [34] observed a correlation between HSI and POD activity in several bands, including orange, red, and NIR spectra, their methodology is not well described and the study lacked control samples of noninfected material. Last, HSI may also be utilized to quantify *B. cinerea*. Liu *et al.* [35] demonstrated that HSI can quantify *B. cinerea* colonies in peach, suggesting that partial least squares (PLS) regression analysis is a robust method for predicting colony counts of *B. cinerea*. In the earlier-mentioned papers, it should be noted that when these changes are not linked to compounds that hallmark specific aspects of resistance or susceptibility, such associations could easily be lost when other cultivars or other environmental conditions are used. Although MSI and HSI can effectively monitor and detect *B. cinerea* infections and distinguish between healthy and infected plant tissues, utilizing them to monitor changes in leaf or fungal metabolites could further enhance our understanding of the infection and defense responses, unlocking their full potential.

3D imaging

3D imaging involves capturing detailed 3D structures of plants using techniques such as laser scanning, stereo cameras, or photogrammetry [36]. This allows precise analysis of plant traits including shape, size, and growth patterns, as well as how these traits can impact or be impacted by pathogen interactions with the plant [37,38]. There are reports on the use of 3D imaging to analyze the architecture of grape bunches; for instance, a loose grape bunch retains less humidity and dries faster after rain, creating less favorable conditions for infections. Using 3D imaging, Herzog *et al.* [39] monitored the 3D architecture and diameter of grape bunches, identifying QTLs related to *B. cinerea* resistance in grapevines. Rist *et al.* [40] measured grape bunches with a 3D scanner in both field and laboratory settings. By implementing a high-throughput 3D imaging pipeline for the automated and objective analysis of individual grape bunch architecture, they were able to predict important phenotyping traits to identify QTLs. However, no studies have specifically focused on the impact of *B. cinerea* on plant organs. Further research is needed to fully leverage this technology, potentially by integrating it with other methods to address the limitations of 2D imaging, such as hidden structures and incomplete architectural perspectives.

Tomography

In addition to the earlier-mentioned techniques, **computed tomography (CT)** and optical coherence tomography (OCT) are promising techniques. OCT uses NIR light and low-coherence interferometry to capture high-resolution images of tissue microstructures. CT uses X-rays taken from multiple angles, which are then combined by a computer to create detailed cross-sectional images.

CT can visualize variations in tissue density, allowing the production of 3D images of plant organ internal structures down to the nanoscale (< 1 μm). This nondestructive technique can be useful to monitor *B. cinerea* infection especially at an early phase of the infection (phase 1 and 2, Figure 1). X-ray CT has been used by Weiller *et al.* [41] to follow the progression of *B. cinerea* infection on grapes and measure changes in the grape density over time that would be linked to tissue degradation. Tomography also has the potential to detect *Botrytis* spp. damage within onion bulbs, as demonstrated by Speir and Haidekker [42] and by Ford *et al.* [43] with, respectively, X-ray CT and OCT. Tomography enables the visualization of internal damage caused by pathogens and shows significant potential for early pathogen detection. However, to the best of our knowledge, only a limited number of studies have used tomography to monitor *B. cinerea* infection in plants.

Challenges and perspectives

Although imaging is a powerful tool for monitoring *B. cinerea*, its capacity for diagnosis is limited, as it is unable to reliably identify *B. cinerea* in naturally occurring infections. However, when combined with other techniques, such as molecular methods, it becomes a valuable asset. For advanced breeding and disease management strategies, challenges are increasingly tied to the limitations of phenotyping efficiency. Visual assessment remains the most commonly used method, but it can delay the implementation of effective management strategies. Furthermore, the availability of large sets of standardized and annotated quantitative data is essential for the development and application of AI and ML approaches [44]. Integrating these technologies is a critical step toward automation. To fully unlock the potential of imaging phenotyping, several key considerations, outlined in the following sections, must be addressed.

Selecting sensor spectral resolution/spatial resolution

To fully realize the potential of imaging techniques, selecting the optimal sensor for specific goals is essential, although this process also presents unique challenges in data integration, accuracy, and scalability. Since *B. cinerea* affects a diverse array of plants and organs, selecting the right imaging protocol and region of interest (ROI) is challenging. Digital imaging methods can be applied across hosts and organs, but settings must be tailored to account for the specific morphological and physiological characteristics of the interaction, particularly for early detection (phase 1 and 2). High-resolution imaging is optimal for monitoring early disease phases (1 and 2) at the infection site. We recommend categorizing pixel values rather than averaging data to detect subtle and highly localized changes. In later phases (3 and 4), when symptoms are more pronounced, imaging can be conducted monitoring larger regions of the plant with correspondingly lower spatial resolution.

Selecting sensors for detection during late phases (3 and 4)

For disease detection and lesion size quantification (phases 3 and 4), RBG imaging is an effective strategy to study the interaction and resistance levels, especially in leaves. However, when applied to non-green plant organs such as fruits, petals, or leaves of varying colors, RGB imaging becomes more challenging in accurately measuring *B. cinerea* lesions due to the limited contrast of chlorotic and necrotic areas. In such cases, thermal and fluorescence imaging offer useful alternatives, either alone or in combination with RGB (Figure 2). While low chlorophyll content and reduced photosynthetic activity in fruits and flowers may limit the effectiveness of these methods, CI remains highly valuable for detecting disease and stress in leaves. While thermal imaging alone is not ideal for detecting *B. cinerea* due to potential inaccuracies under environmental stress, it can enhance RGB imaging. Alternatively, MSI and HSI are better suited for non-green tissues.

Selecting sensors for early detection (phases 1 and 2)

For early detection (phases 1 and 2), CI and HSI are among the most promising methods. CI sensors are highly sensitive and can detect subtle changes in chlorophyll levels before necrosis becomes

visible. In addition, HSI provides a more detailed analysis by predicting changes in plant compounds, such as carbohydrates and phenolics, which are associated with infection [33]. Although complex surface textures, like waxy fruit coatings, can interfere with HSI accuracy, advances in sensor technology and data processing, including multi-angle imaging, are mitigating these challenges. In clustered fruit, where the darker, humid center can encourage pathogen growth, these techniques also help to improve detection precision. Moreover, genes that hallmark specific phases or aspects of the interaction can be used to create indicator plants and *B. cinerea* strains with reporter tags, signaling when key pathways are activated [45,46]. These genetic markers can support early detection and quantify specific infection components through, for example, qPCR.

Image analysis in production systems

By utilizing these methods, we can analyze images to detect patterns and predict potential outbreaks, enabling timely and targeted interventions that reduce production losses related to *B. cinerea*. Analyzing data in production systems comes with additional challenges; the observed stress responses may not be specific to the pathogen interaction, posing a challenge in differentiating between stress due to, for instance, *B. cinerea* and other stress types. Nevertheless, knowledge on the infection process and other metadata on the production system associated with infection risks and disease expression (humidity, light conditions, developmental stage) potentially linked with detection methods on specific locations are likely to quickly identify infections in production systems. In addition, early detection of *B. cinerea* in fruit is challenging, as the infection can remain latent until ripening.

Image analysis for breeding purposes

Inaccuracies from visual observations can slow the detection of QTLs or result in broader QTLs with lower effects, reflected by lower LOD (logarithm of the odds) scores. This, hinders efforts to improve resistance to *B. cinerea*. Furthermore, plant resistance to this pathogen is typically quantitative and highly polygenic, with each gene contributing a small to medium effect. Identifying these genes is complicated by their interaction within epistatic networks, as demonstrated in *A. thaliana* [47]. Digital phenotyping and sensor technology can enhance QTL detection accuracy and reveal complex genetic interactions, aiding resistance-breeding efforts.

Application for other pathosystems

While we focus here on *B. cinerea*, the same digital phenotyping techniques apply to other plant pathogens, in particular for those for which the infection process resembles one or more phases that we defined. This is the case for other necrotrophic plant pathogens such as *Alternaria solani* and *Sclerotinia sclerotium*. In our experience, this review can provide a roadmap for other necrotrophic and even (hemi)biotrophic pathogens [48,49]. The specific details of each step and disease symptoms can vary among different pathogens, and optimization of the balance of digital phenotyping imaging methods or the selected wavelengths is likely to be required for each specific pathosystem.

Concluding remarks

In this review we explored the potential for camera-based digital phenotyping to study the interaction between *B. cinerea* and its hosts, while identifying knowledge gaps in this field. The earlier-mentioned literature shows promise for digital phenotyping in the detection, quantification, and classification of disease symptoms, advancing our understanding of *B. cinerea* infection, and facilitating breeding for resistance and disease management strategies.

Several considerations arise in the switch from visual observations to digital phenotyping, including determining the necessary resolution, automating the imaging process, and establishing

Outstanding questions

Can the 3D aspects of imaging be integrated in digital phenotyping?

How can digital sensor-based phenotyping be used to distinguish between the mechanisms and the associated hallmarks of the infection process?

Can high-resolution imaging such as confocal microscopy and tomography be automated to become applicable for high throughput?

optimal time intervals for observation. As discussed earlier, chlorophyll fluorescence, tomography, and (hyper)spectral imaging are reliable methods for early *B. cinerea* detection, linking disease progression to plant physiological changes. Time-lapse imaging enhances dynamic monitoring of disease development.

Challenges remain, however, including the management of plant 3D structure, automation of processes, and the development of efficient data analysis methods, especially through ML and AI **classifiers** (see Outstanding questions). Plant digital phenotyping is an emerging field, developing rapidly. Its potential in advancing plant science, precision agriculture, and crop productivity is increasingly recognized by researchers, breeders, and growers. Plant digital phenotyping development is fueled by advances in technology and increased computational capabilities including ML and AI. Ultimately, digital phenotyping in combination with complementary omics and molecular technologies will allow quantitative analyses of *B. cinerea* infection and processes that affect susceptibility and resistance through space and time. Understanding the interaction between *B. cinerea* and its host and resulting phenotyping data will advance early detection, enable higher throughput, and provide more robust and reliable results.

Acknowledgments

We thank Rick van de Zedde for his input on the review and support, and Bas Briaire and Najim El Harchioui for their help with HSI and thermal imaging. We acknowledge Ministry of Agriculture, Fisheries, Food Security and Nature for funding via the LWV20335 Phenotyping 4 Profit project and the companies Enza Zaden, Syngenta, KWS, Naktuinbouw, Royal van Zanten, East West Seed, and HBBC as partners in this project.

Declaration of interests

No interests are declared.

Declaration of generative AI and AI-assisted technologies in the writing process

The authors utilized ChatGPT to improve readability and English language use during preparation of the review. After using this tool, the authors reviewed and edited the content as required and take full responsibility for the publication's content.

References

1. Garfinkel, A.R. (2021) The history of *Botrytis* taxonomy, the rise of phylogenetics, and implications for species recognition. *J. Phytopathol.* 111, 437–454
2. Elad, Y. *et al.* (2016) Plant hosts of Botrytis spp. In *In Botrytis – the fungus, the pathogen and its management in agricultural systems* (Fillinger, S. and Elad, Y., eds), pp. 413–486, Springer
3. Dean, R. *et al.* (2012) The top 10 fungal pathogens in molecular plant pathology. *Mol. Plant Pathol.* 13, 414–430
4. Sofianos, G. *et al.* (2023) Multiple and multidrug resistance in *Botrytis cinerea*: molecular mechanisms of MLR/MDR strains in Greece and effects of co-existence of different resistance mechanisms on fungicide sensitivity. *Front. Plant Sci.* 14, 1273193
5. Hahn, M. (2014) The rising threat of fungicide resistance in plant pathogenic fungi: *Botrytis* as a case study. *J. Chem. Biol.* 7, 133–141
6. Bika, R. *et al.* (2021) Botrytis cinerea management in ornamental production: a continuous battle. *Can. J. Plant Pathol.* 43, 345–365
7. Bilkiss, M. *et al.* (2019) Advanced diagnostic approaches for necrotrophic fungal pathogens of temperate legumes with a focus on *Botrytis* spp. *Front. Microbiol.* 10, 1889
8. Denby, K.J. *et al.* (2004) Identification of *Botrytis cinerea* susceptibility loci in *Arabidopsis thaliana*. *Plant J.* 38, 473–486
9. Fu, Y. *et al.* (2017) Genetic mapping and QTL analysis of *Botrytis* resistance in *Gerbera hybrida*. *Mol. Breed.* 37, 13
10. Soltis, N.E. *et al.* (2019) Interactions of tomato and *Botrytis cinerea* genetic diversity: parsing the contributions of host differentiation, domestication, and pathogen variation. *Plant Cell* 31, 502–519
11. Bi, K. *et al.* (2023) Killing softly: a roadmap of *Botrytis cinerea* pathogenicity. *Trends Plant Sci.* 28, 211–222
12. Stewart, E.L. and McDonald, B.A. (2014) Measuring quantitative virulence in the wheat pathogen *Zymoseptoria tritici* using high-throughput automated image analysis. *Phytopathology* 104, 985–992
13. Sankaran, S. *et al.* (2010) A review of advanced techniques for detecting plant diseases. *Comput. Electron. Agric.* 72, 1–13
14. Gowen, A. and Polder, G. (2020) The hype in spectral imaging. *J. Spectr. Imaging* 33, 12–14
15. Tanner, F. *et al.* (2022) Sensor-based phenotyping of above-ground plant–pathogen interactions. *Plant Methods* 18, 35
16. Baranowski, P. *et al.* (2015) Hyperspectral and thermal imaging of oilseed rape (*Brassica napus*) response to fungal species of the genus *Alternaria*. *PLoS One* 10, e0122913
17. Chaerle, L. *et al.* (2007) Early detection of nutrient and biotic stress in *Phaseolus vulgaris*. *Int. J. Remote Sens.* 28, 3479–3492
18. Jafari, M. *et al.* (2017) Detection of pre-symptomatic rose powdery-mildew and gray-mold diseases based on thermal vision. *Infrared Phys. Technol.* 85, 170–183
19. Ha, S.T.T. *et al.* (2023) Early detection of *Botrytis cinerea* infection in cut roses using thermal imaging. *Plants (Basel)* 12, 4087
20. Koh, J.C. *et al.* (2021) Automated machine learning for high-throughput image-based plant phenotyping. *Remote Sens.* 13, 858
21. Lee, U. *et al.* (2018) An automated, high-throughput plant phenotyping system using machine learning-based plant segmentation and image analysis. *PLoS One* 13, e0196615
22. Dolatabadian, A. *et al.* (2024) Image-based crop disease detection using machine learning. *Plant Pathol.*, Published online September 27, 2024. https://doi.org/10.1111/ppa.14006

23. Corwin, J.A. *et al.* (2016) The quantitative basis of the *Arabidopsis* innate immune system to endemic pathogens depends on pathogen genetics. *PLoS Genet.* 12, e1005789
24. Fordyce, R.F. *et al.* (2018) Digital imaging combined with genome-wide association mapping links loci to plant–pathogen interaction traits. *Plant Physiol.* 178, 1406–1422
25. Bhujel, A. *et al.* (2022) Detection of gray mold disease and its severity on strawberry using deep learning networks. *J. Plant Dis. Prot.* 129, 579–592
26. Eizner, E. *et al.* (2017) Characterization of *Botrytis*–plant interactions using PathTrack© – an automated system for dynamic analysis of disease development. *Mol. Plant Pathol.* 18, 503–512
27. Xiao, J.R. *et al.* (2020) Detection of strawberry diseases using a convolutional neural network. *Plants (Basel)* 10, 31
28. Berger, S. *et al.* (2004) Complex regulation of gene expression, photosynthesis and sugar levels by pathogen infection in tomato. *Physiol. Plant.* 122, 419–428
29. Meng, L. *et al.* (2020) Phenotypic variation of *Botrytis cinerea* isolates is influenced by spectral light quality. *Front. Plant Sci.* 11, 1233
30. Wang, H. *et al.* (2018) A method of high throughput monitoring crop physiology using chlorophyll fluorescence and multispectral imaging. *Front. Plant Sci.* 9, 407
31. Pavicic, M. *et al.* (2021) Image-based methods to score fungal pathogen symptom progression and severity in excised *Arabidopsis* leaves. *Plants (Basel)* 10, 158
32. Fahrentrapp, J. *et al.* (2019) Detection of gray mold leaf infections prior to visual symptom appearance using a five-band multispectral sensor. *Front. Plant Sci.* 10, 628
33. Siedliska, A. *et al.* (2018) Detection of fungal infections in strawberry fruit by VNIR/SWIR hyperspectral imaging. *Postharvest Biol. Technol.* 139, 115–126
34. Kong, W. *et al.* (2014) Fast detection of peroxidase (POD) activity in tomato leaves which infected with *Botrytis cinerea* using hyperspectral imaging. *Spectrochim. Acta A Mol. Biomol. Spectrosc.* 118, 498–502
35. Liu, Q. *et al.* (2020) Quantitative visualization of fungal contamination in peach fruit using hyperspectral imaging. *Food Anal. Methods* 13, 1262–1270
36. Paulus, S. (2019) Measuring crops in 3D: using geometry for plant phenotyping. *Plant Methods* 15, 103
37. Paturkar, A. *et al.* (2021) Making use of 3D models for plant physiognomic analysis: a review. *Remote Sens.* 13, 2232
38. Fernandez, R. *et al.* (2024) End-to-end multimodal 3D imaging and machine learning workflow for non-destructive phenotyping of grapevine trunk internal structure. *Sci. Rep.* 14, 5033
39. Herzog, K. *et al.* (2022) Towards sensor-based phenotyping of physical barriers of grapes to improve resilience to *Botrytis* bunch rot. *Front. Plant Sci.* 12, 808365
40. Rist, F. *et al.* (2019) Combination of an automated 3D field phenotyping workflow and predictive modelling for high-throughput and non-invasive phenotyping of grape bunches. *Remote Sens.* 11, 2953
41. Weiller, F. *et al.* (2021) Tracking cell wall changes in wine and table grapes undergoing *Botrytis cinerea* infection using glycan microarrays. *Ann. Bot.* 128, 527–543
42. Speir, R.A. and Haidekker, M.A. (2017) Onion postharvest quality assessment with X-ray computed tomography – a pilot study. *IEEE Instrum. Meas. Mag.* 20, 15–19
43. Ford, H. *et al.* (2011) Investigation of disease in stored onions using optical coherence tomography. In *ISHS Acta Horticulturae 945: IV International Conference Postharvest Unlimited 2011*, ISHS
44. Shakoor, N. *et al.* (2017) High throughput phenotyping to accelerate crop breeding and monitoring of diseases in the field. *Curr. Opin. Plant Biol.* 38, 184–192
45. Cui, F. *et al.* (2019) Cell death regulation but not abscisic acid signaling is required for enhanced immunity to *Botrytis* in *Arabidopsis* cuticle-permeable mutants. *J. Exp. Bot.* 70, 5971–5984
46. Leroch, M. *et al.* (2013) Transcriptome profiling of *Botrytis cinerea* conidial germination reveals upregulation of infection-related genes during the prepenetration stage. *Eukaryot. Cell* 12, 614–626
47. Rowe, H.C. and Kliebenstein, D.J. (2008) Complex genetics control natural variation in *Arabidopsis thaliana* resistance to *Botrytis cinerea*. *Genetics* 180, 2237–2250
48. Barbacci, A. *et al.* (2020) Rapid identification of an *Arabidopsis* NLR gene as a candidate conferring susceptibility to *Sclerotinia sclerotiorum* using time-resolved automated phenotyping. *Plant J.* 103, 903–917
49. Van De Vijver, R. *et al.* (2020) In-field detection of *Alternaria solani* in potato crops using hyperspectral imaging. *Comput. Electron. Agric.* 168, 105106
50. Murchie, E.H. and Lawson, T. (2013) Chlorophyll fluorescence analysis: a guide to good practice and understanding some new applications. *J. Exp. Bot.* 64, 3983–3998
51. Shaw, M.W. *et al.* (2016) Analysis of cryptic, systemic *Botrytis* infections in symptomless hosts. *Front. Plant Sci.* 7, 625
52. Barnes, S.E. and Shaw, M.W. (2003) Infection of commercial hybrid *Primula* seed by *Botrytis cinerea* and latent disease spread through the plants. *J. Phytopathol.* 93, 573–578
53. Sowley, E.N.K. *et al.* (2010) Persistent, symptomless, systemic, and seed-borne infection of lettuce by *Botrytis cinerea*. *Eur. J. Plant Pathol.* 126, 61–71
54. Dewey, F.M. *et al.* (2013) Lateral-flow devices to rapidly determine levels of stable botrytis antigens in table and dessert wines. *Am. J. Enol. Vitic.* 64, 291–295
55. Dewey, F. *et al.* (2000) Quantification of *Botrytis* in grape juice determined by a monoclonal antibody-based immunoassay. *Am. J. Enol. Vitic.* 51, 276–282
56. Fan, X. *et al.* (2015) Development of PCR-based assays for detecting and differentiating three species of *Botrytis* infecting broad bean. *Plant Dis.* 99, 691–698
57. Sanzani, S.M. *et al.* (2012) Early detection of *Botrytis cinerea* latent infections as a tool to improve postharvest quality of table grapes. *Postharvest Biol. Technol.* 68, 64–71
58. Emmanuel, C.J. *et al.* (2022) Microscope studies of symptomless growth of *Botrytis cinerea* in *Lactuca sativa* and *Arabidopsis thaliana*. *Plant Pathol.* 72, 564–581
59. Edwards, S.G. and Seddon, B. (2001) Selective media for the specific isolation and enumeration of *Botrytis cinerea* conidia. *Lett. Appl. Microbiol.* 32, 63–66
60. Simon, U.K. *et al.* (2013) High resolution imaging of temporal and spatial changes of subcellular ascorbate, glutathione and H_2O_2 distribution during *Botrytis cinerea* infection in *Arabidopsis*. *PLoS One* 8, e65811
61. Williamson, B. *et al.* (1995) Effect of humidity on infection of rose petals by dry-inoculated conidia of *Botrytis cinerea*. *Mycol. Res.* 99, 1303–1310
62. Blanco-Ulate, B. *et al.* (2014) Genome-wide transcriptional profiling of *Botrytis cinerea* genes targeting plant cell walls during infections of different hosts. *Front. Plant Sci.* 5, 435
63. Müller, T. *et al.* (2024) Plant infection by the necrotrophic fungus *Botrytis* requires actin-dependent generation of high invasive turgor pressure. *New Phytol.* 244, 192–201
64. Zhu, W. *et al.* (2023) *Botrytis cinerea* BcCDI1 protein triggers both plant cell death and immune response. *Front. Plant Sci.* 14, 1136463
65. Veloso, J. and van Kan, J.A. (2018) Many shades of grey in *Botrytis*–host plant interactions. *Trends Plant Sci.* 23, 613–622
66. Elad, Y. *et al.* (2007) *Botrytis* spp. and diseases they cause in agricultural systems – an introduction. In *Botrytis: biology, pathology and control*, pp. 1–8, Springer
67. Bristow, P. *et al.* (1986) Infection of strawberry flowers by *Botrytis cinerea* and its relevance to grey mould development. *Ann. Appl. Biol.* 109, 545–554
68. Prusky, D. and Lichter, A. (2007) Activation of quiescent infections by postharvest pathogens during transition from the biotrophic to the necrotrophic stage. *FEMS Microbiol. Lett.* 268, 1–8
69. Kuźniak, E. and Skłodowska, M. (2005) Fungal pathogen-induced changes in the antioxidant systems of leaf peroxisomes from infected tomato plants. *Planta* 222, 192–200
70. Kuźniak, E. and Skłodowska, M. (1999) The effect of *Botrytis cinerea* infection on ascorbate–glutathione cycle in tomato leaves. *Plant Sci.* 148, 69–76

71. Vaštakaitė-Kairienė, V. *et al.* (2021) Determination of specific parameters for early detection of *Botrytis cinerea* in lettuce. *Horticulturae* 8, 23
72. Calo, L. *et al.* (2006) Leaf hairs influence phytopathogenic fungus infection and confer an increased resistance when expressing a *Trichoderma* alpha-1,3-glucanase. *J. Exp. Bot.* 57, 3911–3920
73. Zhang, Y. *et al.* (2020) The roles of different types of trichomes in tomato resistance to cold, drought, whiteflies, and *Botrytis*. *Agronomy* 10, 411
74. Aragon, W. *et al.* (2021) *Arabidopsis thaliana* cuticle composition contributes to differential defense response to *Botrytis cinerea*. *Front. Plant Sci.* 12, 738949
75. Liu, R. *et al.* (2023) Ursolic acid, the main component of blueberry cuticular wax, inhibits *Botrytis cinerea* growth by damaging cell membrane integrity. *Food Chem.* 415, 135753
76. Camarillo-Castillo, F. *et al.* (2021) High-resolution spectral information enables phenotyping of leaf epicuticular wax in wheat. *Plant Methods* 17, 58
77. Wang, Y. *et al.* (2021) A rapid detection method for tomato gray mold spores in greenhouse based on microfluidic chip enrichment and lens-less diffraction image processing. *Foods* 10, 3011
78. Ha, S.T.T. *et al.* (2021) Regulation of *Botrytis cinerea* infection and gene expression in cut roses by using nano silver and salicylic acid. *Plants (Basel)* 10, 1241
79. Pignon, C.P. *et al.* (2021) Phenotyping stomatal closure by thermal imaging for GWAS and TWAS of water use efficiency-related genes. *Plant Physiol.* 187, 2544–2562
80. Hou, X. *et al.* (2022) Ultrastructural observations of *Botrytis cinerea* and physical changes in resistant and susceptible grapevines. *Phytopathology* 112, 387–395
81. Elad, Y. and Evensen, K. (1995) Physiological aspects of resistance to *Botrytis cinerea*. *J. Phytopathol.* 85, 637–643
82. Meng, L. *et al.* (2019) Leaf age and light quality influence the basal resistance against *Botrytis cinerea* in strawberry leaves. *Environ. Exp. Bot.* 157, 35–45